01 Jun 2008

Optimal Neuro-Controller Synthesis for Variable-Time Impulse Driven Systems

Xiaohua Wang

S. N. Balakrishnan
Missouri University of Science and Technology, bala@mst.edu

Recommended Citation

X. Wang and S. N. Balakrishnan, "Optimal Neuro-Controller Synthesis for Variable-Time Impulse Driven Systems," *American Control Conference*, Institute of Electrical and Electronics Engineers (IEEE), Jun 2008. The definitive version is available at https://doi.org/10.1109/ACC.2008.4587088

2008 American Control Conference
Westin Seattle Hotel, Seattle, Washington, USA
June 11-13, 2008

Optimal Neuro-Controller Synthesis for Variable-time Impulse Driven Systems

Xiaohua Wang and S. N. Balakrishnan, *Member, IEEE*

***Abstract*—This paper develops a systematic scheme to solve for the optimal controls of variable time impulsive systems. First, the optimality conditions for variable time impulse driven systems are derived using the calculus of variation. After wards, a neural network based adaptive critic method is proposed to numerically solve the two-point boundary value problems formulated based on the optimality conditions derived. Finally, two examples-one linear and one nonlinear-are presented to illustrate the conditions derived and to show the power of the neural network based adaptive critic method proposed.**

I. Introduction

Many dynamic processes are characterized by the fact that, at certain moments of time, they experience a abrupt change of states. Since the duration of change is negligible in comparison with the duration of the process, it is natural to assume that these changes are in the form of impulses.

There have been applications of impulsive control in chaotic systems [1-3], biped walking robots [4], optimal fixed time fueling process [5], biological control [6], financial and economics control [7-8], and satellite formation control [9-10]. There are many other examples in practice such as ultra high speed optical signals over communication networks, collision of particles, inventory control, government decisions, interest changes, and stock price changes etc. Brogliato [11] describes modeling and dynamics of the impulsive actions. Several others [12-16] investigate the basic problems such as existence of the solutions and system stability. Haddad et al. [17] examine the stability of impulsive systems using dissipativity. Xie and Wang [18] study the conditions for controllability and observability of impulsive systems.

There are two types of impulse driven systems [12, 16]. One with impulse times fixed, is called the fixed time impulsive system. The optimality control of this kind of impulsive system has been studied in the authors' previous paper [19], where several theorems have been presented on the linear fixed-time optimal impulsive control. The other type is the variable time impulsive system. In this type of system, the instants impulse times are not fixed, but are functions of the states. Impulses are will not be activated until certain "resetting conditions" conditions are satisfied.

For the purpose of studying the impulsive control, in this paper, impulses are the only control available to the system and there is no continuous control. Therefore, the system here is addressed as impulse driven system instead of general impulsive system.

Though the literature on impulsive control is quite extensive, still there exists a need for the development of systematic impulsive control design methods. This paper develops an optimal impulse-driven controller technique that satisfies those needs. Furthermore, the proposed neural network based technique does not require abnormal assumptions and is implementable.

The rest of the paper is organized as follows. Section II contains the derivation of the necessary conditions for optimality. Section III illustrates the special neural network scheme based on a structure called "single network adaptive critic (SNAC)''. Section IV presents two illustrative problems and the simulation results. The case studies consist of results from a linear problem and a nonlinear problem. Finally, section V provides the conclusions.

II. Optimal Impulse Control

A. Problem Formulation

In this paper, the following variable time impulse driven system is considered, with the system model given by

$$\begin{cases} \dot{x} = f_c(x) & G\left(x\left(\tau_i^-\right)\right) \neq 0 \\ x_i^+ = h\left(x_i^-, u_i\right) \triangleq x_i^- + g_d\left(x_i^-\right) u_i & G\left(x\left(\tau_i^-\right)\right) = 0 \end{cases} \tag{1}$$

where $x \in \mathbb{R}^{n\times 1}$. $f_c(x) \in \mathbb{R}^{n\times 1}$ is Lipchitz continuous. $g_d(x)$ is continuous differentialable. δ is a dirichlet function. $u_i = \int_{\tau_i^-}^{\tau_i^+} u_i \delta(t-\tau_i)\,dt$. $u_i \in \mathbb{R}^{m\times 1}$. $i = 1,2,3,\ldots,\mathbb{Z}^+$. $0 \le \tau_i < \infty$ are instants when impulses are given, satisfying the resetting condition

$$G\left(x\left(\tau_i^-\right)\right) = 0 \tag{2}$$

τ_i's are also referred to as impulse instants hereafter. Initial states x_0 and initial time are assumed to be known. Note that impulse control u_i is the only control applied to the system (1) and that no continuous control is included.

In this study, a fairly general cost function for minimization is considered as follows.

Manuscript received September 13, 2007. This work was supported in part by the NSF Grant ECS-0601706.

Xiaohua Wang is a PhD student with Department of Aerospace and Mechanical Engineering, University of Missouri, Rolla, MO 65401 USA. (Email: wxw98@umr.edu)

S. N. Balakrishnan is a professor with Department of Mechanical and Aerospace Engineering, University of Missouri, Rolla, MO 65401 USA. (Email: bala@umr.edu. Tel: 573-341-4675. Fax: 573-341-4607)

$$J = \Phi(x_f) + \sum_{i=1}^{k} L_d(u_i) + \sum_{i=1}^{k+1} \int_{\tau_{i-1}^+}^{\tau_i^-} L_c(x)dt \tag{3}$$

where $\Phi(x_f)$ is the constraint on the terminal states, $\sum_{i=1}^{k} L_d(u_i)$ is the penalty on the impulse control, and $\sum_{i=1}^{k+1} \int_{\tau_{i-1}^+}^{\tau_i^-} L_c(x_i)dt$ is the penalty on the piecewise continuous states. Note that $\tau_{k+1}^- = t_f$, where t_f is the final time.

B. Optimality Conditions

Theorem 1: Given system dynamics as in (1) with known initial time and initial states, a resetting condition as in (2), a cost function as in (3), and assuming the optimal control exists, by introducing the Hamiltonian function [30]

$$H \triangleq L_c(x) + \lambda^T f_c(x) \tag{4}$$

the necessary conditions for the optimality are presented in the following equations.

1) At $t = t_f$,

$$\lambda_f^T = \frac{\partial \Phi(x_f)}{\partial x_f} \tag{5}$$

2) For $t \in \left[\tau_i^+, \tau_{i+1}^-\right]$,

- State propagation equation is

$$\dot{x} = f_c(x) \tag{6}$$

- Costate propagation equation is

$$\frac{\partial H(x)}{\partial x} + \dot{\lambda}^T = 0 \tag{7}$$

3) Between pre impulse and post impulse, $t \in \left[\tau_i^-, \tau_i^+\right]$,

- State update equation is

$$x_i^+ = x_i^- + g_d(x_i^-)u_i \tag{8}$$

- Costate update equation is

$$\lambda^T(t_i^-) - \lambda^T(t_i^+)\left(I + \frac{\partial g_d(x_i(t_i^-))}{\partial x_i}u_i\right) + \mu\frac{\partial G}{\partial x_i^-} = 0 \tag{9}$$

- Resetting equation is

$$G\left(x\left(\tau_i^-\right)\right) = 0 \tag{10}$$

- Control equation is

$$\frac{\partial L_2(u_i)}{\partial u_i} + \lambda^T(t_i^+)\, g_d\left(x_i(t_i^-)\right) = 0 \tag{11}$$

- Jump equation is

$$H_i^+ = H_i^- \tag{12}$$

Proof:

Using Hamiltonian function (4), the objective function (3) can be rewritten as

$$J = \Phi(x_f) + \sum_{i=1}^{k} L_d(u_i) + \sum_{i=1}^{k+1} \int_{\tau_{i-1}^+}^{\tau_i^-} \left(H(x) - \lambda^T \dot{x}\right)dt \tag{13}$$

where $\tau_{k+1}^- = t_f$.

Suppose u_i is the optimal control and that x is the optimal state. By introducing a set of multipliers γ_i and μ, the optimal cost function can then be written as

$$\begin{aligned} J_0 = {} & \Phi(x_f) + \sum_{i=1}^{k}\left[L_d(u_i) + \mu G\left(x_i^-\right)\right] \\ & + \sum_{i=1}^{k}\gamma_i\left[h(x_i^-, u_i) - x_i^+\right] + \sum_{i=1}^{k+1}\int_{\tau_{i-1}^+}^{\tau_i^-}\left[H(x) - \lambda^T\dot{x}\right]dt \end{aligned} \tag{14}$$

Now, perturb control u_i by letting $u_i \to u_i + \varepsilon n_i$, impulsive instants $\tau_i \to \tau_i + \varepsilon\theta(t)$, then the corresponding $x \to x + \varepsilon\eta(t)$. The cost function after perturbation is written as follows.

$$\begin{aligned} J_\varepsilon = {} & \Phi(x_f + \varepsilon\eta_f) + \sum_{i=1}^{k}\left[L_d(u_i + \varepsilon n_i) + \mu G\left(x\left(t_i^- + \varepsilon\theta_i\right) + \varepsilon\eta_i^-\right)\right] \\ & + \sum_{i=1}^{k}\gamma_i\left[h\left(\left(x\left(t_i^- + \varepsilon\theta_i\right) + \varepsilon\eta_i^-\right), u_i + \varepsilon n_i\right) - x\left(t_i^+ + \varepsilon\theta_i\right) - \varepsilon\eta_i^+\right] \\ & + \sum_{i=1}^{k+1}\int_{\tau_{i-1}^+ + \varepsilon\theta_{i-1}}^{\tau_i^- + \varepsilon\theta_i}\left[H(x+\varepsilon\eta) - \lambda^T\left(\dot{x} + \varepsilon\dot{\eta}\right)\right]dt \end{aligned} \tag{15}$$

The last term on the right hand side of (15) can be rewritten as follows.

$$\begin{aligned} & \sum_{i=1}^{k+1}\int_{\tau_{i-1}^+ + \varepsilon\theta_{i-1}}^{\tau_i^- + \varepsilon\theta_i}\left[H(x+\varepsilon\eta) - \lambda^T\left(\dot{x} + \varepsilon\dot{\eta}\right)\right]dt \\ & = \sum_{i=1}^{k+1}\int_{\tau_{i-1}^+ + \varepsilon\theta_{i-1}}^{\tau_{i-1}^+} + \int_{\tau_{i-1}^+}^{\tau_i^-} + \int_{\tau_i^-}^{\tau_i^- + \varepsilon\theta_i}\left[H(x+\varepsilon\eta) - \lambda^T\left(\dot{x} + \varepsilon\dot{\eta}\right)\right]dt \\ & = \sum_{i=1}^{k+1}\left(\int_{\tau_{i-1}^+ + \varepsilon\theta_{i-1}}^{\tau_{i-1}^+} + \int_{\tau_i^-}^{\tau_i^- + \varepsilon\theta_i} L_c dt\right) + \int_{\tau_{i-1}^+}^{\tau_i^-}\left[H(x+\varepsilon\eta) - \lambda^T\left(\dot{x} + \varepsilon\dot{\eta}\right)\right]dt \\ & = \sum_{i=1}^{k+1}\left(\left(L_c\right)_i^-\varepsilon\theta_i - \left(L_c\right)_{i-1}^+\varepsilon\theta_{i-1}\right) + \int_{\tau_{i-1}^+}^{\tau_i^-}\left[H(x+\varepsilon\eta) - \lambda^T\left(\dot{x} + \varepsilon\dot{\eta}\right)\right]dt \end{aligned} \tag{16}$$

Because the initial conditions are known, the corresponding variations at the initial time are zeros. Rearrange the first term of the last line on the right hand side of (16),

$$\sum_{i=1}^{k+1}\left(\left(L_c\right)_i^-\varepsilon\theta_i - \left(L_c\right)_{i-1}^+\varepsilon\theta_{i-1}\right) = \sum_{i=1}^{k}\left(\left(L_c\right)_i^- - \left(L_c\right)_i^+\right)\varepsilon\theta_i \tag{17}$$

Equation (16) becomes

$$\begin{aligned} & \sum_{i=1}^{k+1}\int_{\tau_{i-1}^+ + \varepsilon\theta_{i-1}}^{\tau_i^- + \varepsilon\theta_i}\left[H(x+\varepsilon\eta) - \lambda^T\left(\dot{x} + \varepsilon\dot{\eta}\right)\right]dt \\ & = \sum_{i=1}^{k}\left(\left(L_c\right)_i^- - \left(L_c\right)_i^+\right)\varepsilon\theta_i + \int_{\tau_{i-1}^+}^{\tau_i^-}\left[H(x+\varepsilon\eta) - \lambda^T\left(\dot{x} + \varepsilon\dot{\eta}\right)\right]dt \end{aligned} \tag{18}$$

Once the last term on the right-hand side of (18) is integrated by part, equation (18) can be written as

$$\begin{aligned} & \sum_{i=1}^{k+1}\int_{\tau_{i-1}^+ + \varepsilon\theta_{i-1}}^{\tau_i^- + \varepsilon\theta_i}\left[H(x+\varepsilon\eta) - \lambda^T\left(\dot{x} + \varepsilon\dot{\eta}\right)\right]dt \\ & = \sum_{i=1}^{k+1}\left(\left(L_c\right)_i^- - \left(L_c\right)_i^+\right)\varepsilon\theta_i + \sum_{i=1}^{k+1}\int_{\tau_{i-1}^+}^{\tau_i^-}\left(\frac{\partial H}{\partial x} + \dot{\lambda}^T\right)\varepsilon\eta dt - \sum_{i=1}^{k+1}\varepsilon\lambda^T\eta\Big|_{\tau_{i-1}^+}^{\tau_i^-} \end{aligned} \tag{19}$$

Since $\delta J = \lim_{\varepsilon \to 0} \frac{J - J_0}{\varepsilon}$, the first order approximation of the perturbed cost J_ε can be written as

$$\begin{aligned}
\delta J &= \frac{\partial \Phi(x_f)}{\partial x_f}\eta_f \\
&+\sum_{i=1}^{k}\left[\frac{\partial L_d(u_i)}{\partial u_i}n_i + \mu\frac{\partial G\left(x_i^-\right)}{\partial x_i^-}\eta_i^- + \mu\frac{\partial G\left(x_i^-\right)}{\partial x_i^-}\dot{x}_i^-\theta_i\right] \\
&+\sum_{i=1}^{k}\gamma_i\left[\frac{\partial h}{\partial x_i^-}\eta_i^- + \frac{\partial h}{\partial x_i^-}\dot{x}_i^-\theta_i + \frac{\partial h}{\partial u_i}n_i - \dot{x}_i^+\theta_i - \eta_i^+\right] \\
&+\sum_{i=1}^{k+1}\left(\left(L_c\right)_i^- - \left(L_c\right)_i^+\right)\theta_i \\
&+\sum_{i=1}^{k+1}\int_{\tau_{i-1}^+}^{\tau_i^-}\left(\frac{\partial H}{\partial x} + \dot{\lambda}^T\right)\eta dt - \sum_{i=1}^{k+1}\lambda^T\eta\Big|_{\tau_{i-1}^+}^{\tau_i^-}
\end{aligned} \tag{20}$$

Considering that initial conditions are known($\eta_0 = 0$), the last term on the right hand side of (20) is rewritten as

$$-\sum_{i=1}^{k+1}\lambda^T\eta\Big|_{\tau_{i-1}^+}^{\tau_i^-} = \sum_{i=1}^{k}\left(\lambda_i^{+T}\eta_i^+ - \lambda_i^{-T}\eta_i^-\right) - \lambda_f{}^T\eta_f \tag{21}$$

Substituting (21) into (20) and rearranging terms, equation (20) can be written as follows.

$$\begin{aligned}
\delta J &= \left(\frac{\partial \Phi(x_f)}{\partial x_f} - \lambda_f^T\right)\eta_f + \sum_{i=1}^{k}\left[\frac{\partial L_d(u_i)}{\partial u_i} + \gamma_i\frac{\partial h}{\partial u_i}\right]n_i \\
&+\sum_{i=1}^{k}\left[\left(\mu\frac{\partial G\left(x_i^-\right)}{\partial x_i^-} + \gamma_i\frac{\partial h}{\partial x_i^-} - \lambda_i^{-T}\right)\eta_i^- + \left(\lambda_i^{+T} - \gamma_i\right)\eta_i^+\right] \\
&+\sum_{i=1}^{k+1}\int_{\tau_{i-1}^+}^{\tau_i^-}\left(\frac{\partial H}{\partial x} + \dot{\lambda}^T\right)\eta dt \\
&+\sum_{i=1}^{k}\left(\gamma_i\left(\frac{\partial h}{\partial x_i^-}\dot{x}_i^- - \dot{x}_i^+\right) + \mu\frac{\partial G\left(x_i^-\right)}{\partial x_i^-}\dot{x}_i^- + \left(L_c\right)_i^- - \left(L_c\right)_i^+\right)\theta_i
\end{aligned} \tag{22}$$

Since n_i, θ_i, and η are independent, to eliminate them from influencing δJ, one can choose the multiplier $\lambda(t)$ such that the coefficients of n_i, θ_i, and η_i vanish. Consequently, $\gamma_i = \lambda_i^{+T}$. Also,

$$\dot{\lambda}^T = -\frac{\partial H}{\partial x} \tag{23}$$

$$\left(\lambda_i^-\right)^T = \mu\frac{\partial G\left(x_i^-\right)}{\partial x_i^-} + \lambda_i^{+T}\frac{\partial h}{\partial x_i^-} \tag{24}$$

with the boundary condition

$$\lambda_f^T = \frac{\partial \Phi(x_f)}{\partial x_f} \tag{25}$$

Now, equation (22) becomes

$$\begin{aligned}
\delta J &= \sum_{i=1}^{k}\left[\frac{\partial L_d(u_i)}{\partial u_i} + \gamma_i\frac{\partial h}{\partial u_i}\right]n_i \\
&+\sum_{i=1}^{k}\left(\gamma_i\left(\frac{\partial h}{\partial x_i^-}\dot{x}_i^- - \dot{x}_i^+\right) + \mu\frac{\partial G\left(x_i^-\right)}{\partial x_i^-}\dot{x}_i^- + \left(L_c\right)_i^- - \left(L_c\right)_i^+\right)\theta_i
\end{aligned} \tag{26}$$

For δJ to be zero for any arbitrary n_i and θ_i,

$$\frac{\partial L_2(u_i)}{\partial u_i} + \lambda^T\left(t_i^+\right)g_d\left(x_i\left(t_i^-\right)\right) = 0 \tag{27}$$

$$\gamma_i\left(\frac{\partial h}{\partial x_i^-}\dot{x}_i^- - \dot{x}_i^+\right) + \mu\frac{\partial G\left(x_i^-\right)}{\partial x_i^-}\dot{x}_i^- + \left(L_c\right)_i^- - \left(L_c\right)_i^+ = 0 \tag{28}$$

Condition (28) can be rearranged and written as the jump condition,

$$H_i^+ = H_i^- \tag{29}$$

By rearranging the conditions (23)-(29), all the conditions in theorem 1 are validated. Equation (29) is referred to as the jump equation hereafter.

Remark 1: Assuming initial time, initial states, and initial costates are all given, system states and costates propagate using equations (6) and (7) until the resetting condition $G\left(x\left(\tau_i^-\right)\right) = 0$ is satisfied at time instant τ_i. Considering the state update equation (8), costate update equation (9) and control equation (11), one can calculate variable μ as a function of the states and costates before impulse using the jump equation (12). After μ is calculated, states and costates can propagate forward at the impulse instant and so on until t_f. To help solve the two point boundary value problem, a neural network based numerical method is proposed in the next section.

Remark 2: The instants when impulses are applied are not known in the problem.

Remark 3: Conditions (5)-(12) are valid for the finite horizon optimal control problems. For the infinite time optimization, conditions (6) to (12) are still valid. But the final condition (5) is no longer needed. optimal control problem

III. Solution Technique: SNAC

This section introduces the single network adaptive critic (SNAC) technique which is used in this paper to solve the optimal impulse control problems. SNAC has been used in solving nonlinear control problems in [19]. This paper extends the SNAC scheme to variable time impulse control problems.

A. Adaptive Critic Overview

The concept of adaptive critic is derived from the modeling of the brain as a supervisor and an action structure [19] where the supervisor criticizes the action (controller) of the system to achieve a better overall goal. The novelty of this paper lies in using neural network structures, SNAC, to solve optimal variable time impulse control problems. Note that one can handle both the finite time and the infinite time horizon

problems using this structure. Only the case of the infinite time horizon is presented in this paper.

B. Infinite Time Adaptive Critic Neural Network Scheme

The idea of the SNAC technique is to use the state and the costate propagation equations, the state and costate update equations, the jump equation, and the control expression in (5) -(12) to train a single neural network to capture the optimal relation between costates and states. In this paper, the neural network is trained to approximate the function $\lambda^+(x_i^-)$ with x_i^- as inputs and λ_i^+ as outputs. After that, the costates can be used to calculate optimal control.

Figure 1 gives the flowchart of the optimal impulsive control synthesis using "SNAC". The neural network used is called NN in the picture. x_i^- is a set of states chosen so that its range approximately spans the domain of interest. The NN is initialized based on an initial stabilizing control design, as a function of x_i^-. "i" is used here to index the impulses. In Fig.1, the resetting condition $G(x_i^-)=0$ is necessary to decide when an impulse should happen.

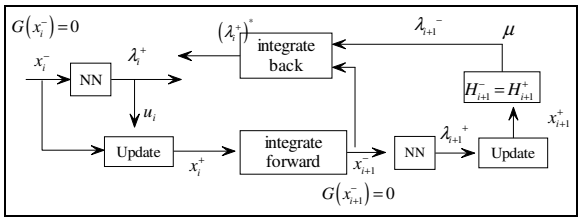

Fig. 1 SNAC Architecture of Infinite Time Horizon Problems

Steps used in the neural network training are:

1) Input x_i^- to the NN to obtain λ_i^+ as the output. With λ_i^+ and x_i^-, use (11) to calculate u_i.

2) Use the calculated u_i and x_i^- in the impulse state update equation (8) to get x_i^+.

3) Propagate the state x_i^+ using equation (6) until the resetting condition (10) is satisfied. Then x_{i+1}^- is calculated at τ_{i+1}.

4) Input x_{i+1}^- to the NN to get λ_{i+1}^+ and calculate u_{i+1}, then calculate x_{i+1}^- using the state update equation (8) to get x_{i+1}^+.

5) Calculate μ through the jump equation (12) by substituting x_{i+1}^-, x_{i+1}^+, λ_{i+1}^-, and λ_{i+1}^+.

6) Calculate $\lambda_{i+1}^{-\,*}$ through the state update equation (8), costate update equation (9), and solved μ.

7) Use equations (6) and (7) to back propagate the states x_{i+1}^- and costates $\lambda_{i+1}^{-\,*}$ and get the target λ_i^{+*}.

8) Train SNAC with x_i^- as the input and λ_i^{+*} as the target output.

9) Stop training when the error between λ_i^{+*} and λ_i^+ is small enough (within an error bound set by the control designer).

IV. Simulation Results

For concept illustration, a linear vector system is considered first, followed by a nonlinear vector example with some similarity to the linear one.

A. Linear Vector Problem

The linear vector problem is an oscillator problem with the following dynamics.

$$\dot{x} = \begin{bmatrix} 0 & 1 \\ -\omega^2 & 0 \end{bmatrix} x + \begin{bmatrix} 0 \\ 1 \end{bmatrix} u_i \delta(t-\tau_i) \tag{30}$$

where $\omega^2 = 60$ and the impulse is activated when the following resetting condition (31) is satisfied.

$$x_1(\tau_i) = 0 \tag{31}$$

Without control, system open loop response is depicted in Fig. 2.

Choose the objective function

$$J = \sum_{i=1}^{k} (u_i^T R u_i) + \sum_{i=1}^{k+1} \int_{\tau_{i-1}^+}^{\tau_i^-} (x^T Q x) dt \tag{32}$$

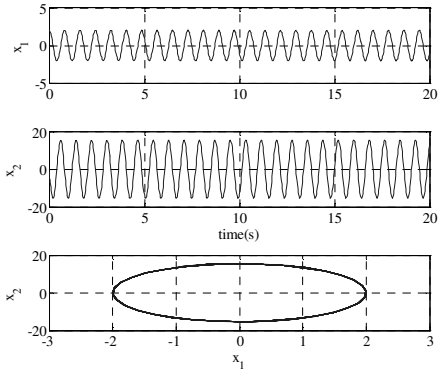

Fig.2 System response without impulsive control

Using the optimality conditions and considering the Hamiltonian function $H = \frac{1}{2}(q_1 x_1^2 + q_2 x_2^2) + \lambda_1 x_2 + \lambda_2(-\omega^2 x_1)$, the states and costates propagation equations between τ_i^+ and τ_{i+1}^- are listed as follows.

$$\begin{cases} \dot{x}_1 = x_2 \\ \dot{x}_2 = -\omega^2 x_1 \\ \dot{\lambda}_1 = -q_1 x_1 + \omega^2 \lambda_2 \\ \dot{\lambda}_2 = -q_2 x_2 - \lambda_1 \end{cases} \tag{33}$$

The state and costate update equations at $t \in [\tau_i^-, \tau_i^+]$ where impulses are applied are as follows.

$$\begin{cases} u_i = -\dfrac{1}{r}\lambda_2^+ \\ \lambda_1^+ = \lambda_1^- - \mu \\ \lambda_2^+ = \lambda_2^- \\ x_1^+ = x_1^- = 0 \\ x_2^+ = x_2^- + u_i \\ H_i^+ = H_i^- \end{cases} \tag{34}$$

Substitute the other optimality conditions in (34) into the last jump equation $H_i^+ = H_i^-$. The parameter μ can be expressed as a function of λ^- and x^-, which is

$$\mu = \frac{\lambda_2^-\left(2q_2 x_2^- r - q_2\lambda_2^- + 2\lambda_1^- r\right)}{2r\left(x_2^- r - \lambda_2^-\right)} \tag{35}$$

Therefore, if substituting μ expression (35) back into (34), the relation between states/costates after impulse and before impulse are known. This relation is used in step 6 during the training process.

Two 1-3-3-1 multilayer perceptron neural networks are used to approximate $\lambda_1^+\left(x_2^-\right)$ and $\lambda_2^+\left(x_2^-\right)$, respectively. The two neural networks are pre-trained as $\lambda_1^+ = 0.5x_2^-$ and $\lambda_2^+ = 0.5x_2^-$. Also, $q_1 = 1$, $q_2 = 1$, and $r = 1$ are chosen.

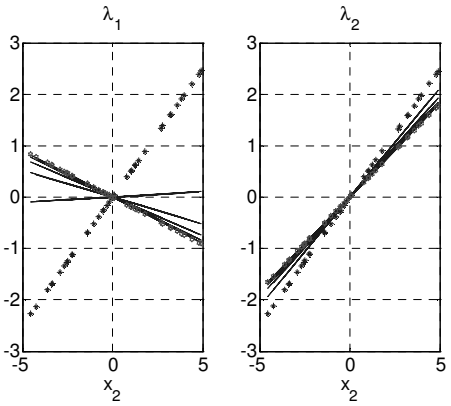

Fig. 3 Convergence of the neural network output

Figure 3 shows the training process of the SNAC scheme. For a set of different points of x_2^-, the outputs start from the line with the star marks and converge upon the line with hexagrams.

To observe the converging process more clearly, since a linear relation between the costate and state exists, assume $\lambda_1^+ = k_1 x_2^-$ and $\lambda_2^+ = k_2 x_2^-$. Figure 4 gives a better view of the training process. From the plot at the top of Fig. 4, the value of the cost function *J* decreases to a constant along the training process. From the two plots at the bottom of Fig. 4, it is easy to see that k_1 and k_2 converge after about 7 iterations to the constants -0.255 and 0.362, respectively. Figure 5 is the system response with the optimal control calculated using SNAC neural networks. The initial states are chosen as $x_0 = [0,\ 3]^T$.

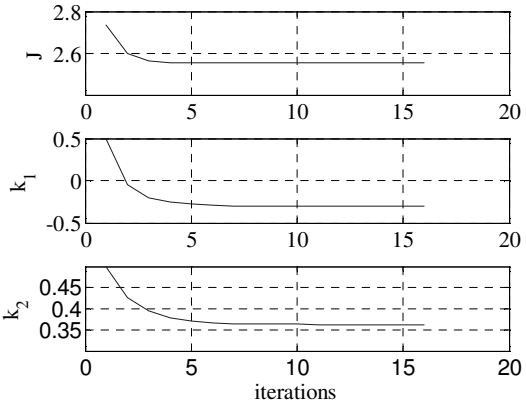

Fig. 4 Convergence of the training process and the change in the objective function

The system is asymptotically stable with the designed optimal control from the plot.

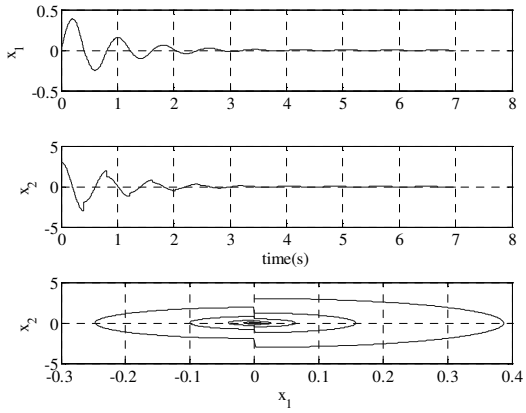

Fig. 5 System response with the optimal impulse control

B. Nonlinear vector example

Consider the following system dynamics

$$\begin{bmatrix} \dot{x}_1 \\ \dot{x}_2 \end{bmatrix} = \begin{bmatrix} x_2 + a\sin(x) \\ -\omega^2 x_1 \end{bmatrix} + \begin{bmatrix} 0 \\ 1 \end{bmatrix} u_i \delta\left(t - \tau_i\right) \tag{36}$$

where $a = 3$ and $\omega^2 = 60$.

Take the same cost function (32) used in the previous example. The resetting condition is also chosen as $x_1\left(\tau_i\right) = 0$. This example is similar to the previous example except that there are nonlinearities in the system dynamics. Figure 6 shows the system open loop response.

Two 1-6-6-1 multilayer perceptron neural networks are used to approximate the relations $\lambda_1^+\left(x_2^-\right)$ and $\lambda_2^+\left(x_2^-\right)$ respectively. The two neural network are also pre-trained using $\lambda_1^+ = 0.5x_2^-$ and $\lambda_2^+ = 0.5x_2^-$. Figure 7 shows the trained neural network output λ_i^+ and the target output $\left(\lambda_i^+\right)^*$ needed in the SNAC training scheme.

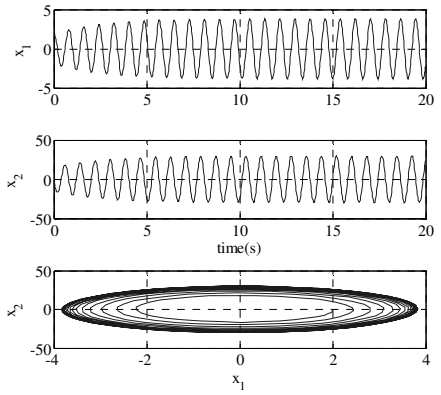

Fig. 6 Openloop system response

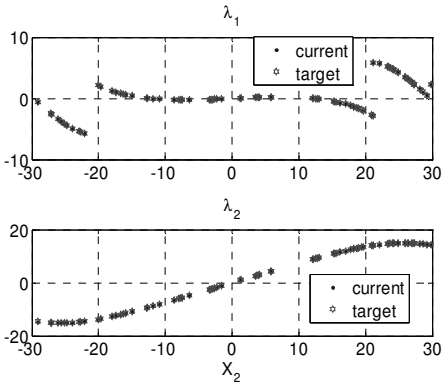

Fig. 7 outputs of the neural network and the target outputs

(λ_i^+ and $\left(\lambda_i^+\right)^*$)

In this figure, the trained output (current) λ_i^+ is very close to the target output (target) $\left(\lambda_i^+\right)^*$.

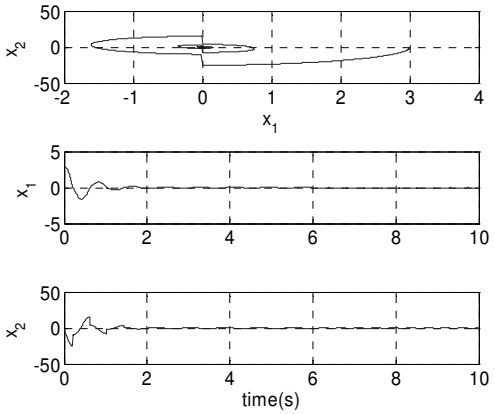

Fig. 8 System response with the controls calculated through trained neural networks.

Figure 8 depicts system closed loop response using the controls calculated from the trained neural networks. The states are decreasing to zeros and are asymptotically stable in the picture.

Remark 4: In this paper, to concentrate on the studies of impulsive control, no continuous control is considered. But the whole scheme presented here, including the condition derivation and the numerical SNAC, can be easily extend to the variable time impulsive control with continuous control.

V. Conclusion

In this paper, the necessary conditions are derived for optimal control of the variable time impulse driven systems. A single neural network adaptive critic (SNAC) method is developed to numerically solve the linear/nonlinear optimal impulsive control problems. The simulation results of a linear impulse problem and a nonlinear problem show the effectiveness of the SNAC scheme. A systematic scheme of the optimal control of impulse driven systems is developed.

References

[1] Guan, Z., Chen, G., and Ueta, T. (2000). On impulsive control of a periodically forced chaotic pendulum system, IEEE Transactions on Automatic Control, 45(9):1724-1727.

[2] Kozlov, A. K.; Osipov, G. V.; Shalfeev, V. D. (1997). Suppressing chaos in continuous systems by impulse control, Control of Oscillations and Chaos, Proc., 1st International Conf., 3: 578-581.

[3] Sun, J. and Zhang, Y. (2004). Impulsive control of Lorenz systems. Intelligent Control and Automation, Fifth World Congress on, 1:71-73.

[4] Grizzle, J. W., Abba, G., and Plestan, F. (2001). Asymptotically stable walking for biped robots: analysis via systems with impulse effects. IEEE Transaction on Automatic Control, 46(1):51-64.

[5] Gilbert, E. and Harasty, G. (1971). A class of fixed-time fuel-optimal impulsive control problems and an efficient algorithm for their solution, IEEE Transactions on Automatic Control, 16(1):1-11.

[6] Lu, Z., Chi, X., and Chen, L. (2003). Impulsive control strategies in biological control of pesticide. Theoretical Population Biology. 64(1):39-47.

[7] Sun, J., Qiao, F. and Wu, Q. (2005), Impulsive control of a financial model. Physics Letters A. 335(4):282-288.

[8] Case, J. H. (1979), Economics and the competitive process, New York, New York University Press.

[9] Vaddi, S. S., Alfriend, K. T., and Vadali, S. R., and Sengupta, P. (2005). Formation establishment and reconfiguration using impulsive control. Journal of Guidance, Control, and Dynamics. 28(2):262-268.

[10] Xin. M., Balakrishnan, S. N. and Pernicka, H. (2004). Deep-Space Spacecraft Formation Flying Using Theta-D Control, AIAA Guidance, Navigation, and Control Conference and Exhibit, Providence, RI.

[11] Brogliato, B. (1996). Nonsmooth impact mechanics: models, dynamics, and control, London, New York : Springer.

[12] Lakshmikantham, V., Bainov, D. D. and Simeonov, P. S. (1989). Theory of impulsive differential equations, Singapore; Teaneck, NJ: World Scientific.

[13] Liu, X. and Siegel, D. (1994). Comparison methods and stability theory, New York : Dekker.

[14] Samoilenko, A. M. and Perestyuk, N. A. (1995). Impulsive differential equations ; (translated from the Russian by Yury Chapovsky) Singapore, River Edge, NJ : World Scientific.

[15] Clarke, F. H. (1998). Nonsmooth analysis and control theory, New York : Springer.

[16] Yang, T. (2001). Impulsive control theory, Berlin, New York , Springer Verlag.

[17] Haddad, W.M., Chellaboina, V. and Kablar, N.A. (1999). Nonlinear Impulsive Dynamical Systems Stability and Dissipativity Part I, Proc. of the 38th Conference on Decision & Control, Phoenix, Arizona USA.

[18] Xie, G. and Wang, L. (2004). Necessary and Sufficient Conditions for Controllability and Observability of Switched Impulsive Control Systems, IEEE Transactions on Automatic Control, 49(6):960-966

[19] Wang, X. and Balakrishnan, S.N. (2007). Optimal Neurocontroller Synthesis for Impulse-Driven Systems, Proceedings of the 2007 American Control Conference, New York City, USA.